MICROSTRAIN AND LOW FREQUENCY HYSTERETIC DISLOCATION DAMPING IN COPPER SINGLE CRYSTALS

D. M. Barnett and J. M. Roberts

ABSTRACT

Current knowledge concerning the early stages of yielding in copper is briefly reviewed. A detailed study of the anelastic limit (τ_A) and low frequency hysteretic damping loss of copper crystals of two levels of impurity (99.999% pure and a Cu-0.01% Al alloy) has been carried out at various prestrains up to a maximum of about 10^{-2}. τ_A and the decrement were found to be independent of temperature in the range 135°K to 300°K for the pure crystals. The amplitude dependence of the decrement became less non-linear with increasing prestrain. The decrement at constant stress amplitude passes through a maximum with prestrain for the Al alloy crystal, but is simply observed to decrease with prestrain for the purer crystals. The decrease in the decrement appears to be related to the onset of stage II hardening in copper. The current hysteresis results, in the frequency range 10^{-1} cps, are in good agreement with previously published results when the internal friction measurements were conducted in the kilocycle frequency range. The present results are discussed qualitatively in terms of the most generally accepted theory for stage II hardening, namely the long range elastic interaction between dislocations originally proposed by Seeger[1]. It is noted that as the strain in stage II proceeds, a friction stress acting upon dislocations increases. The value of this friction stress is not negligible compared with the flow stress, and it is suggested that it should be considered in a theory for stage II hardening. The origin of this friction stress appears to be associated with point defects and also possibly with the jog density of the mobile dislocation lines.

D. M. Barnett, Student Member A.I.M.E., and J. M. Roberts, Member A.I.M.E., are graduate student in Mechanical Engineering and Associate Professor of Mechanical Engineering, respectively, William Marsh Rice University, Houston, Texas.

INTRODUCTION

There exist in the literature[1-7] several theories describing stage II hardening in f.c.c. metals. Oftentimes the data is specifically referred to copper. No simple method has yet been divised to clearly discriminate between these various theories[6]. The mechaism or mechanisms governing the flow stress and work hardening in stage I of copper is quite complicated, yet recent results favor impurities as playing a major role in controlling the flow stress of high purity copper[7]. The latter results indicate that as copper crystals are made more pure, the flow stress decreases and the temperature dependence of the flow stress becomes suppressed to very low temperatures (i.e., about 50°K and below). These results are in complete agreement with Young's suggestion[8] that the yield stress in the elastic to plastic transition region in copper crystals of 99.999% purity is determined by the stress necessary to break the gliding dislocations through impurity atom barriers in the crystal. The dislocation was visualized to move as a rigid rod through the impurity field.

Young[9] has also clearly shown that during the very initial stages of deforming a copper crystal, motion of grown-in dislocations occurs at about 4 gm/mm^2 and dislocation multiplication occurs at stresses as low as 18 gm/mm^2. A significant fact observed by Young[9], however, is that dislocations in these high purity prestrained copper crystals could move backwards as much as one to six microns upon unloading the crystal. These same dislocations had moved between 23 to 35 microns during prestraining. Since Young's observations were of the etch pit type, hence a surface observation, it is possible an image force effect as discussed by Friedel[10] may have played some role in the backward dislocation motion observed. In any event, as long as dislocation motion is restricted in any sense (such as by line tension, the internal stress or a surface image force) in 99.999% pure copper crystals, it appears that reverse dislocation motion may occur to a considerable extent.

Tinder and Washburn[11] have studied polycrystalline OFHC copper at various impurity levels of Al and Fe in the very initial stages of yielding. They were particularly interested in the very initial motion of dislocations in annealed crystals which caused strains between 10^{-9} to 10^{-7}. The present authors agree that under these conditions, initial loading causes the irreversible movement of dislocations which were probably in almost metastable equilibrium positons either due to line tension, internal stress or the details of dislocation nodal configurations. In the present study, however, the anelastic behavior is studied after various known prestrains have been introduced into the crystal. Under these conditions, the effects of the movement of the very few dislocations studied by Tinder and Washburn[11] have been removed. Prestraining enables one to obtain reproducible microstrain data as well as data which may be correlated to that of other investigators, such as the macroscopic properties of the specimen.

Of fundamental importance to the understanding of the plastic flow and pre-yield phenomena of any metal is a clear understanding of the temperature dependence of its flow stress and the stress dependence of its pre-yield delay time. It appears from the work of Blewitt, et. al.[12,13] and Köster[7] that 99.999% copper single crystals grown in vacuum do not exhibit a temperature dependence of the flow stress between 77 to 300°K. The temperature dependence of the 2×10^{-6} plastic yield point in 99.999% pure copper and 99.97 OFHC copper observed by Rosenfield and Averbach[14] was indeed rather weak. The authors mention that the temperature dependence of the 2×10^{-6} yield stress which they observed was only somewhat higher than the temperature dependence of the elastic constants. In fact, if one removes the temperature dependence of the elastic constants[15] from their polycrystalline specimen results, then the 2×10^{-6} microyield point is temperature independent. Within the experimental accuracy of the data of Rosenfield and Averbach[14], it is doubtful that one can

conclude that the 2×10^{-6} yield stress in 99.97 OFHC or 99.999% high purity copper does or does not exhibit a true temperature dependence. Liu[16], et. al. found no stress dependent delay time in 99.98 % OFHC copper between 83 to 298°K. This suggests that pre-yield phenomena in copper of even this low purity may be temperature independent. They did find the critical resolved shear stress to be temperature dependent in this region, which is consistent with the results of Diehl and Berner[17] for crystals of the same purity. Kramer[18] found for compressed 99.999% copper crystals a stress dependent delay time in the temperature range 82 to 298°K. He found evidence for $\{123\}$ type slip, and attributed the delay time results to this event. If no $\{123\}$ type slip occurs in 99.999% pure copper crystals, then it appears to date that pre-yield phenomena is primarily temperature independent.

The strain amplitude, frequency and temperature dependence of the internal friction in the kilocycle range of about 99.98% pure copper single crystals was studied by Nowick[19]. The temperature dependent effects observed by Nowick suggested thermal unpinning of dislocations from impurities as a possible origin. Nowick concludes, however, that the predominant mechanism appears to be one of hysteresis loss, whereby dislocations tear over energy barriers from one position to another with negligible thermal assistance.

Weertman and Koehler[20] working with 99.999% copper single crystals found the decrement in the kilocycle frequency range to pass through a maximum with compressional prestrain. Hasiguti and Hirai[21] have previously observed this effect in electrolytic copper crystals. They pointed out that the maximum in the decrement curve with prestrain appears to correspond to the transition region between stage I and stage II. Weertman and Koehler[20] found Young's modulus to continuously decrease as the decrement passed through its maximum. Nowick[22] suggests that the decrease of the true modulus is probably due to the decrease in the average interatomic force constants as a result of the deformation. Increasing amplitude

of the long range internal stresses with prestrain would be compatible with this concept. Weertman and Koehler[20] also found the decrement to be strongly amplitude dependent at strain amplitudes above several times 10^{-7}. The strength of the amplitude dependence decreased with increasing prestrain. They interpreted a portion of these results in the light of a dislocation oscillating as a vibrating string which was acted upon by a restoring force due to the elastic interaction with neighboring dislocations and impurity atoms. The strong amplitude dependence was suggested to be associated with the dislocation overcoming impurity or any other barriers not associated with the elastic interaction of dislocations. The peak of the decrement versus prestrain curve was attributed to the increased dislocation density with prestrain, and their formal relations for the amplitude independent decrement verified this. The explanation proposed by Weertman and Koehler[20] for their results is in complete agreement with the suggestion of Nowick[19].

In the present paper the authors have sought for correlations between the macroscopic stress strain behavior and low frequency damping[23] in copper crystals of 99.999% purity. Low frequency measurements were deemed necessary to allow a direct comparision with the plastic flow behavior. The temperature and prestrain dependence of the anelastic limit (τ_A)[24,25] as well as its relationship to the macroscopic stress-strain curve has also been studied to further assist an understanding. The results are discussed in rather general terms with respect to dislocation theories in an attempt to bring consistency to the known plastic behavior of copper in its early stages of deformation.

EXPERIMENTAL PROCEDURE

Cylindrical single crystals, 0.5 in. in dia. and approximately 7.5 in. long, were grown from 99.999% pure ASARCO copper. The crystals were grown in a split graphite crucible under vacuum using a modified Bridgman technique. Each crystal was then cut in

half, and slightly oversized cylindrical aluminum grips were fixed to both specimens with Shell Epon Adhesive VI. All crystals were chemically polished prior to testing. The orientations of the specimens tested, including an 0.01 atomic % aluminum alloy crystal (CM-Al), are shown in Figure 1.

Simple tension tests were conducted using an Instron testing machine. The Instron load cell signal was applied to the Y-input of a Moseley X-Y Recorder. A capacitance gauge extensometer[26] was used in conjunction with a Fielden Proximity Meter[26] capacitance bridge to provide the strain signal to the X-axis of the X-Y recorder. In this manner load-displacement (or essentially resolved shear stress - resolved shear strain curves) could be permanently recorded.

During room temperature testing, 3.5 in. O.D. thin-walled yellow brass tubing shielded the specimen and pull-rod assembly from air currents which tended to cause local temperature variations detectable by the capacitance gauge. The same tubing served to shield the specimen from the isopentane cooling medium used for low temperature tests. Liquid nitrogen was introduced through cooling coils suspended in the isopentane cooling bath, and equilibrium was attained at temperatures below room temperature by balancing the liquid nitrogen flow rate with the power output from a Thermotrol* temperature control system. Three iron-constantan thermocouples were located along the crystal, so that the specimen temperature could be recorded. The experimental technique and method of calibration is essentially the same as that employed by Roberts and Hartman.[23,25] Stresses are accurate to $\pm$ 1.5 gm/mm^2 and strains from + 13% to -8% in the microstrain region for all temperatures investigated.

---

* Hallikainen Instruments, 1341 Seventh St., Berkeley 10, California

No hysteresis loops were observable until each specimen was subjected to small prestrains. Figure 2 schematically depicts typical results obtained from a prestrain test. The specimen was prestrained to a stress τ_p corresponding to a plastic prestrain γ_p. It will be noted that γ_p is purely plastic strain, as the elastic strain contribution has been subtracted out in these calculations. After prestraining, linear load-unload curves were observed at small stress amplitudes. At higher stress amplitudes closed hysteresis loops were noted until an open loop first appeared at a stress level denoted as τ_A.[24,25] The stress amplitude at which a given loop was measured is denoted by τ_o. The specimen was then further prestrained, and hysteresis loops were again measured as a function of τ_o until an open loop was first noted. In this manner the crystals were incrementally prestrained to about 1% resolved shear strain, and hysteresis loops were measured at each prestrain. All prestrain tests were performed at room temperature. Crystal CM-2T was prestrained at room temperature until hysteresis loops judged large enough to be measurable were observed. Temperature was then decreased in increments of about 25°C, and hysteresis loops, as well as τ_A, were measured (without further prestrain) as a function of temperature in the range 135-300°K.

A copper -0.01 atomic percent aluminum alloy single crystal CM-Al was also grown and prestrain-tested at room temperature in an attempt to determine an impurity effect.

EXPERIMENTAL RESULTS AND ANALYSIS

The decrement Δ is defined in this study in exactly the same manner as by Roberts and Brown.[27] The most difficult portion of the analysis of the experimental data was the determination of the decrement with a minimum of error. Δ is merely a ratio of two areas and is thus independent of strain calibration. Since the hysteresis loops observed

in copper were quite small, planimetering proved to be highly unsatisfactory for an accurate analysis of the data. A graphical method, depicted schematically in Figure 3, was found to be more suitable.

The hysteresis loops could be subdivided into a series of n triangles and trapezoids as shown. If w_i denotes the width of the loop at the i^{th} incremental division, then the area of the loop, W_{irr}, is given by

$$W_{irr} = h \sum_{i=1}^{n-1} w_i \tag{1}$$

where h is the constant incremental stress subdivision. The total work input W_T was analyzed in a similar manner. If a vertical line is drawn from the top of the loop to the horizontal axis, and if b_i denotes the horizontal distance from this vertical line to the loading portion of the loop, then

$$W_T = h \left\{ 1/2 \; b_o + \sum_{i=1}^{n-1} b_i \right\} \tag{2}$$

The decrement, or W_{irr}/W_T, is thus seen to be independent of h. Error in decrement data using this scheme is almost entirely due to error in determining w_i, the loop width. It is estimated that for small loops measured at low stress amplitudes the error in Δ is about 10%. At higher stress amplitudes where the loops are larger in size, the error is about 3-5%.

All stresses and strains reported are quantities resolved on the most favored slip system. Table I lists the geometrical trigometric factors for each crystal along with the calculated[15] and observed elastic moduli. In Table I, θ is the angle between the specimen axis and the normal to the $\{111\}$ type slip plane and ϕ is the angle between the specimen axis and the $\langle 110 \rangle$ slip direction predicted to operate on the $\{111\}$ planes. It is noted that θ and ϕ are given for the two most favored slip systems. It was found

that the very initial modulus for the crystals tested was within 10% of that predicted from isothermal elastic constant data obtained by the pulse-echo technique. The observed modulus is consistently low, suggesting dislocation bowing in copper of this purity from about zero stress. Using data obtained from the room temperature prestrain tests, it was possible to reconstruct stress-strain curves for each specimen tested. Figure 4 shows two such reconstructed curves; one for the copper -0.01 atomic % aluminum alloy crystal, and one for a 99.999% copper crystal. One notes the increased flow stress level for the alloyed specimen. All reconstructed stress-strain curves were characterized by the absence of an extended easy glide region. The absence of a persisting easy glide region is believed to be due to the large diameter crystals employed in this study[28] as well as the small difference between the $\cos\theta \cos\phi$ factors as noted in Table I.

The prestrain dependence of τ_A, the stress necessary to create an open hysteresis loop, is recorded in Figure 5 for both a pure and the alloy crystal. τ_A is always less than τ_p, and $\tau_A(\gamma_p)$ closely resembles the stress-strain curve, $\tau_p(\gamma_p)$.

The prestrain dependence of the decrement for a given stress amplitude in both a pure and the alloy crystal is recorded in Figures 6 and 7. For the purer crystal at prestrains $>$ 0.2% (which corresponds to the region of stage II hardening as is seen from Figure 4) the decrement is always decreasing as a function of prestrain. One notes that the magnitude of the decrement change with prestrain is very large compared with any possible errors inherent in the calculation of Δ.

The decrement is seen to increase with prestrain in the stage I - stage II transition region ($\gamma_p < 0.3\%$) for the alloy crystal. Since the impurity additions raised the flow stress (see Figure 4), closed hysteresis loops which increased with prestrain could

TABLE I

Orientation of Crystals Tested and Observed and Calculated Young's Moduli

Crystal	θ (deg)	ϕ (deg)	$\cos\theta \cos\phi$	E(calculated) $gm/mm^2 \times 10^{-6}$	E(observed) $gm/mm^2 \times 10^{-6}$
CM-1	53 31	38 62	0.48 0.40	10.3	10.2
CM-2	47 32	44 59	0.49 0.44	9.85	9.28
CM-4	52 52	45 52	0.44 0.39	13.8	12.7
CM-5	60 68	33 29	0.42 0.35	17.2	17.0
CM-AL	50 32	40 61	0.49 0.42	9.95	8.05

be detected at stress amplitudes at which only open loops would have been observed in the purer crystal. However, once the alloy crystal had been prestrained into stage II, Δ again decreased with prestrain. The stress amplitude dependence of the decrement also decreased with prestrain (Figure 8). At prestrains near 1% Δ is a shallow, almost linear function of τ_o.

Low temperature investigations indicated that both τ_A and Δ were temperature insensitive from 135°K to 300°K for the purer crystal (Figure 9). The error in measuring τ_A is about 5% and hence is within the limit of detecting a change in τ_A through a temperature variation of the elastic constants. Prior to the low temperature tests, the existence of any possible time effect upon τ_A and Δ was investigated over a six hour period. No such effect was found.

Hysteretic internal friction is characterized by an average frictional stress $\bar{\tau}_F$ which is defined in the following manner. Since W_{irr} represents an energy loss, this loss may be expressed in the form

$$W_{irr} = \oint \bar{\tau}_F \, d\gamma''_B \tag{3}$$

where γ''_B is the anelastic strain out of phase with the applied stress by $\pi/2$. γ''_B is assumed proportional to the dislocation strain γ_B (Figure 2), and the contour integral is taken conterclockwise around the hysteresis loops. If γ_{BL} represents the dislocation strain measured from the initial modulus line to the loading portion of the loop and γ_{BU} is the dislocation strain measured from the modulus line to the unloading segment of the loop, then:

$$W_{irr} = \int_o^{\tau_o} \bar{\tau}_F \, d\gamma_{BU} - \int_o^{\tau_o} \bar{\tau}_F \, d\gamma_{BL}$$

$$= \int_o^{\tau_o} \bar{\tau}_F \, d(\gamma_{BU} - \gamma_{BL})$$

$$= \int_o^{\tau_o} \bar{\tau}_F \, dw_L \tag{4}$$

where w_L is the loop width expressed in resolved shear strain units. Since the loops are very nearly symmetrical about w_L (maximum) which occurs at approximately one-half the stress amplitude τ_o,

$$W_{irr} = 2 \int_o^{w_L(max.)} \bar{\tau}_F \, dw_L = \text{a function of } w_L(max.)$$

Thus, from elementary integral calculus,

$$\frac{dW_{irr}}{dw_L(max.)} = 2\bar{\tau}_F = \text{slope of } W_{irr} \text{ vs. } w_L(max.) \text{ curve.}$$

Figure 10 is a plot of W_{irr} vs. w_L(max.) at various prestrains for crystal CM-1T. The curves are not quite linear, although there may be errors in w_L(max.) of 10 to 15%. $\bar{\tau}_F$ may be computed from the average slopes, and these results are shown in Figure 11 for both a pure and the alloy single crystals.

DISCUSSION

The first important point to note is the remarkable similarity between the present results and those studies of the prestrain dependence of the internal friction in the kilocycle range[19,20,21] carried out by earlier investigators. It must be noted, however, that the lowest values of the decrement (about 0.03 to 0.01) observed in the present study are about the highest values observed by the previous workers. The point defect-dislocation interaction mechanism for internal friction in prestrained copper at low frequencies as described by Okuda and Hasiguti[29] is believed to cause a relaxation strength too small to be detected by the techniques used in the present study. Fig. 8 clearly shows Δ to be temperature independent in the range studied, and hence predominantly a hysteresis type loss is clearly indicated. The main facts which must be explained are:

(1) That the decrement appears to rise in the easy glide region and then pass through a maximum as one enters stage II hardening. (Fig. 7)

(2) The low frequency hysteretic decrement is strongly amplitude dependent after very mild prestrains, yet becomes less amplitude dependent as one passes into stage II hardening. (Fig. 9)

(3) The anelastic limit (τ_A) appears to follow the stress-strain curve and appears to be temperature independent in the range investigated. (Figs. 5 & 8)

The authors wish to suggest a possible qualitative explanation for the present results. The decrement is given by

$$\Delta = \frac{\oint \bar{\tau}_F \, d\gamma''_B}{\int_0^{\gamma_T} \tau \, d\gamma_T} \tag{5}$$

where

$$\gamma_T = \gamma_E + \gamma'_B + \gamma''_B \tag{6}$$

γ_E is the elastic shear strain, γ'_B the plastic strain in phase with the applied stress τ, and γ''_B the plastic strain out of phase with τ by $\pi/2$. This definition is then in qualitative agreement with the suggestions of Nowick[19] and Weertman and Koehler[20] that the amplitude dependent loss is associated with dislocation tearing over impurity barriers or the like. $\bar{\tau}_F$ is an average frictional stress resisting dislocation motion.[30,31] Also, $\gamma_B = \gamma'_B + \gamma''_B$, and since γ''_B is assumed proportional to the loop width, γ'_B is in general greater than γ''_B (Fig. 2) except at very low stresses. γ_E was found to be anywhere from 6 to 20 times γ_B. The $\int_0^{\gamma_T} \tau \, d\gamma_T$ at constant τ_o was found to be almost independent of prestrain. Therefore the decrement passing through a maximum or continuously decreasing with prestrain is primarily due to changes in $\oint \bar{\tau}_F \, d\gamma''_B$ since $\gamma_E + \gamma'_B > \gamma''_B$. It is assumed that γ''_B is proportional to ρ (the dislocation density) and $\bar{x}$, the

average distance moved by dislocation.

The authors believe that a dominant portion of $\bar{\tau}_F$ is given by

$$\bar{\tau}_F = \sum_{i=1}^{n} \frac{c_i U_i}{n} \qquad (7)$$

where c_i is the number of point defects per unit volume of type i and U_i the interaction energy of the i^{th} species with a dislocation. The details of an essentially athermal frictional stress existing between dislocations moving through random impurities have been treated theoretically recently by Takamura and Morimoto[32] and Ookawa and Yazu[33]. These calculations are quite complicated, and yet in each case the frictional drag force depends linearly on the concentration of impurities and other constant factors which are weakly temperature dependent. Both these groups of authors[32,33] place numerical values into their resulting equations for a Cu -10% Zn alloy and obtain reasonable values for its flow stress. *We suggest, that the latter detailed theoretical calculations lend* support to the use of an athermal frictional stress of the type given by equation (7).

The frictional stress was observed in the present study to increase with prestrain. Strut[31] observed $\bar{\tau}_F$ in a copper crystal to more than double after 500 cycles of cyclic straining at amplitudes of about 10^{-4}. He attributed this rise to an enhanced concentration of point defects as a consequence of a large cumulative cyclic strain. This is a possible explanation for the increase of $\bar{\tau}_F$ with prestrain in the present study, since rather large concentrations of vacancies, namely 10^{-4} to 10^{-7}, may form after about 1% deformation in copper.[34,35] In the present study, however, $\bar{\tau}_F$ increases rapidly with small prestrains (see Fig. 11) and an additional type of lattice friction may be introduced. $\bar{\tau}_F$ for pure copper increases by a factor of almost five for a prestrain of 6.5×10^{-3} (Fig. 11). The prestrain dependence may have an additional origin other than an enhanced

point defect concentration. During prestraining, dislocations cut other dislocations and an increased jog density is formed on dislocations lying in the active $\{111\}$ planes. The conformity planes[36] of these jogs will depend upon the Burgers vectors of the intersected and intersecting dislocations and may be expected to be of the $\{100\}$ or $\{110\}$ type. In general, this will probably give rise to a glide conformity plane which requires a stress τ_j larger than that required for slip of the unjogged dislocation. If jogs of this type are spaced by a distance ℓ_j and b is the Burgers vector of the dislocation, then it is readily shown that an incremental increase in the frictional stress is given by

$$\Delta \bar{\tau}_F = \tau_j \frac{b}{\ell_j} \tag{8}$$

for continued motion of the dislocation. This additional frictional stress would then have to be added to equation (7). As long as these jogs do not exist in pure screw dislocations, some restricted conservative motion of these dislocations is permissible. If these jogs exist in pure edge dislocations, then their motion is unrestricted as far as generation of point defects is concerned. Equation (8) suggests the average frictional stress would increase as ℓ_j decreases, that is, as strain proceeds. We cannot exclude, however, that the vacancy concentration will increase with strain and also contribute to the increase of $\bar{\tau}_F$. The authors are not able to discriminate between these two possible mechanisms.

We now wish to qualitatively explain the three facts pointed out at the beginning of this discussion with the preceeding concepts in mind. τ^*, the effective stress acting upon dislocation, will be given by

$$\tau^* = \left[\tau - \tau_G(\gamma_p, \bar{x}) - \bar{\tau}_F(\gamma_p) \right] \tag{9}$$

where τ is either τ_o (the stress amplitude of a loop) or the applied stress, τ_G is the

long range internal stress field and $\bar{\tau}_F$ is as previously described. τ_G and τ_F are strong functions of the prestrain or prior stress but are only very weak functions of temperature. The manner in which τ^* may vary with the average dislocation displacement $\bar{x}$ at various prestrains γ_p is schematically shown in Fig. 12. It must be emphasized that Fig. 12 merely respresents a schematic type of τ^* versus $\bar{x}$ curve which would seem to agree with the present results. Detailed studies relating these quantities have been made[5,20] and it is clear the resulting relations depend upon the number of near neighbor dislocations taken specifically into account as well as the fact that both long range and short range elastic interactions are considered. Fig. 13 shows the relation between $\bar{x}$ and τ^* when the constant line tension approximation is employed (using the exact expression for the radius of curvature of the dislocation) and the dislocation is assumed to bow out between two strong pinning points of separation distance 2ℓ. α is a constant equal to about 1[9] for prestrained crystals, G is the shear modulus, and b the Burgers vector.

To qualitatively explain the behavior of Δ and τ_A with prestrain, one must examine the behavior of $\bar{\tau}_F$, τ_G, and γ''_B during stage I and stage II hardening. In stage I, where very little secondary slip is observed, γ''_B will be given by

$$\gamma''_B \propto \rho_p b \bar{x} \tag{10}$$

where ρ_p is the dislocation density on the primary slip planes. During stage I, Young[8] has shown that the dislocation density in high purity copper can increase by a factor of about 20 (from 10^5 to 2×10^6 cm^{-2}) for a stress increase of about 25 gms/mm^2. Since τ_G (max) is assumed related to τ_A, which changes only by a factor of 1.5 during easy glide, it is highly probable that the increased density of primary dislocations dominates any

increase of τ_G or $\bar{\tau}_F$ with prestrain in stage I. Hence, prior to stage II, the anelastic strain γ''_B increases through ρ_p at about constant $\bar{x}$, and thus Δ initially increases with prestrain at constant τ_o.

The maximum in the Δ versus γ_p curve is observed in the impure crystal, but not in the purer specimens (Figs. 6 and 7). For the purer crystals in stage I, irreversible dislocation motion occurs at low values of stress, so that $\tau_G + \bar{\tau}_F$ is probably of the order of τ_o, and hence τ^* and likewise $\bar{x}$ approach zero. Therefore, hysteresis loops cannot be observed within the limits of the current detection system. Furthermore, after small prestrains, the long dislocation loops l which experience the largest force are assumed to move; hence it is possible that the mobile dislocations move over the non-linear portion of the τ^* vs. $\bar{x}$ plots of Figs. 12 and 13. Prior to stage II a strong non-linear amplitude dependence of the decrement may be expected, as Fig. 8 indicates.

It should be pointed out that the authors cannot distinguish between that portion of the hysteresis loops associated with restricted dislocation motion such as shown schematically in Figs. 12 and 13 when $\tau^* < \tau_A$, and that portion due to unrestricted dislocation motion. It seems reasonable to assume, however, that the relative amount of unrestricted motion should decrease as the prestrain increases (at constant value of the applied stress) and hence should be in qualitative agreement with a decreasing decrement with prestrain. Therefore the enhanced dislocation density on the primary plane appears to be the dominant effect giving rise to the decrement increase in the impure crystal at small prestrains. This explanation is in agreement with the presentation by Shvidkovsky et. al.[36] in describing a rather similar behavior observed in NaCl and and LiF crystals.

As one enters stage II hardening, the stress-dislocation density relation becomes

much stronger[8] such that $\tau_p \simeq 2 \times 10^{-4} \rho^{0.85}$ in stage II. If τ_A is assumed proportional to $\rho^{1/2}$ [1-7], then (τ_A / τ_p) is approximately $\propto \tau_p^{-0.4}$. The decrease of (τ_A / τ_p) with prestrain or τ_p is readily observable for the pure crystal in Fig. 5. For the impure crystal, the stress-dislocation density relationship appears to be less strong than that for the pure crystal, at least in the very early stage of deformation.

It should be pointed out that Livingston[39] found the stress-dislocation density relation to be almost parabolic, $\tau_p = \frac{Gb\rho^{1/2}}{3}$ for a wide range of crystal orientations over the high stress region 100 to 10,000 gm/mm^2. The work by Young[8] explores the details of the stress-dislocation density relation over the low stress region covered by the present investigation. Furthermore, Livingston[39] does observe some deviation from the parabolic law at the lower stresses. The present authors believe Young's data is more applicable to the current work after very small prestrains and comparitively low stresses than is an extrapolation of the data of Livingston.

An important point to remember is that the microstrain measurements and the anelastic behavior (whether in the kilocycle or the very low frequency range) closely resembled the macroscopic flow behavior. Hence some correlation between microstrain, anelastic data, and macroscopic flow theories should exist. The recent work of Schoeck[38] and Hirsch[40] lends credibility to the long range internal stress field work-hardening theory proposed by Seeger[1] for the stage II hardening. τ_G (max) may include the short range elastic interaction discussed by Saada[5,41] and Mitra and Dorn.[42] The current study cannot differentiate between the two. It is encouraging to note that Mitra and Dorn observed the long range internal stress versus plastic strain to follow the stress-strain curve in OFHC copper single crystals. This lends support to the suggestion that τ_A is related to the combined long and short range elastic dislocation interactions. It seems reasonable to relate τ_A to τ_G (max.) and $\bar{\tau}_F$, since the present work indicates that

further forward plastic dislocation strain (i.e. - open loops) would occur at $\tau_A = \tau_G$ (max.) + $\bar{\tau}_F$.

Now upon examining Figures 4, 5, and 11 it is seen that:

(1) τ_A increases by about 90-100 gms/mm^2 for $0.3\% \leq \gamma_p \leq 0.7\%$.

(2) $\bar{\tau}_F$ increases by about 35 gms/mm^2 over the same prestrain interval.

Thus, the internal stress τ_G (max.) has increased by about 60-70 gms/mm^2 in early stage II hardening, which is about twice the change in $\bar{\tau}_F$ over the same prestrain range.

The temperature independence of τ_A (Fig. 9) within an accuracy 5% is in accordance with the interpretation that $\bar{\tau}_F$ is temperature insensitive except for the temperature dependence of the elastic constants, which is also the case of τ_G (max.)

Upon the initiation of stage II deformation, where the dislocation density increases rapidly[8], the dislocation forest density changes and long range elastic interaction between dislocation pileups occurs.[1] Since τ_G (max.) and $\bar{\tau}_F$ are increasing in stage II, $\tau^* = \left[\tau_o - \tau_G - \bar{\tau}_F\right]$ is decreasing (for a fixed τ_o). As τ^* decreases, $\bar{x}$ approaches zero and the $\tau^* - \bar{x}$ functional relation is linear. This relation is linear for small τ^* and $\bar{x}$ in figure 13. For figure 12 one can justify a linear relationship by using a truncated Taylor series or by looking at a detailed model such as was done by Weertman and Koehler[20]. In stage II one qualitatively expects the decrement to decrease with prestrain since $\bar{x}$ decreases and to obey a linear stress amplitude dependence law; this was experimentally observed.

It should be pointed out that the rapid decrement decrease in stage II cannot be simply explained upon a dislocation bowing theory. If the hysteresis loops were simply related to the dislocation bowing which occurs at stresses below those required for Frank-

Read source generation, then

$$\gamma_B'' \propto \rho_p b \bar{x}_p + \rho_s b \bar{x}_s \tag{11}$$

where ρ_p and ρ_s are the dislocation densities on primary and secondary slip systems, and $\bar{x}_p$ and $\bar{x}_s$ the average distance moved during bowing of these dislocations. In general, $\bar{x} \propto \ell^2$ (Fig. 13) and $\rho \propto \ell^{-2}$ (3,43); then γ_B'' would be independent of prestrain and one could not predict a decrease in Δ as a function of γ_p. Clearly the current results indicate that other factors also play an important role. For example ρ is either not a simple reciprocal function of ℓ^2, or $\bar{x}$ is less than that predicted by being proportional to ℓ^2; the latter probably due to the enhanced friction stress and internal stress as strain proceeds in stage II.

It must be emphasized that in no way can the current study specifically discriminate between the various theories for stage II hardening. The authors have considered numerous possibilities and conclude that only if one adopts a specific hysteresis loss model could a unique distinction possibly arise. The latter is not feasible since the relative proportion of line tension limited dislocation motion to that associated with dislocations moving against the internal stress gradient $\tau_G(\bar{x})$ is certainly not known. If one does adopt the view, however, that a good correlation between macroscopic and microscopic flow behaviors has been shown, then the experimental results suggest that the dislocations in stage II experience not only the effects of τ_G, the internal stress, but also a lattice friction stress $\bar{\tau}_F$ which is not negligible with respect to τ_G. $\bar{\tau}_F$ may be due to either jogs or point defects as outlined in the discussion. Simple macroscopic studies probably are not able to discriminate between these two effects, since both τ_G(max.) and $\bar{\tau}_F$ increase with prestrain. The latter thought suggests that stage II hardening

theories as they exist are possibly an oversimplification, since none of these attempt to incorporate both the long range internal stress effect as well as an enhanced lattice friction stress.

SUMMARY

1). The initial stage of yielding in two levels of impurity copper crystals has been studied in detail. After various small prestrains, the anelastic limit (τ_A) and hysteresis loops were studied in detail.

2). τ_A versus prestrain was found to be similar to the stress-strain curve.

3). The stress-strain curve exhibited a very small region of easy glide namely $\leq 5 \times 10^{-3}$ plastic strain. The low frequency hysteresis loss at constant stress amplitude decreased sharply with increasing prestrain in stage II.

4). From the strain amplitude dependence of the hysteresis loops, the average frictional stress resisting dislocation motion was found to increase with prestrain.

5). After small prestrains the stress dependence of the decrement was non-linear. After further prestraining the stress amplitude dependence of the decrement became less non-linear.

6). The current results are in complete agreement with previous anelastic studies made in the kilocycle frequency range. The present results confirm a true hysteretic type loss, since similar observed behaviors now span 4 orders of magnitude of frequency. τ_A and the decrement (hysteretic) were found to be independent of temperature in the range (135 to 300)$^{\circ}$K.

7). The results are qualtiatively discussed in the light of the most favored theory for stage II hardening in copper, namely, the long range elastic interaction of dislocations proposed by Seeger[1]. It appears that the dislocations which move in

stage II experience an enhanced lattice friction stress with increasing prestrain. This friction stress may be associated with an enhanced concentration of either lattice point defects or with an increased jog density on the glissile dislocations. It is suggested that such behavior must be taken into account before a complete theory describing stage II hardening in copper can be obtained.

ACKNOWLEDGMENTS

The authors wish to thank Drs. F. R. Brotzen and W. Pfeiffer of the Mechanical Engineering Department, W. M. Rice University, for many stimulating discussions and for reviewing the manuscript in its early stage. The authors express their thanks to Mr. Robert Herring and Mr. D. E. Hartman for assistance with certain aspects of the experimental work.

The support of the National Aeronautics and Space Administration under Grant NsG-6-59 is gratefully acknowledged.

FIGURE CAPTIONS

Figure 1. Portion of a standard [001] stereographic net showing the pole of the specimen axis for each of the crystals studied.

Figure 2. Schematic stress-strain diagram depicting typical results.

Figure 3. Schematic drawing depicting the graphical method employed to analyze the hysteresis loops.

Figure 4. Stress-strain curves for crystals CM-Al and CM-IT.

Figure 5. (τ_A/τ_p) versus γ_p for crystals CM-Al and CM-IT.

Figure 6. Decrement (Δ) versus γ_p at different stress amplitudes for crystal CM-IT.

Figure 7. Decrement (Δ) versus γ_p at different stress amplitudes for crystal CM-Al.

Figure 8. Decrement (Δ) versus τ_o at different prestrains (γ_p) for crystal CM-IT.

Figure 9. τ_A versus T($^\circ$K) for crystal CM-2T after $\gamma_p = 5 \times 10^{-3}$. Δ versus T($^\circ$K) for crystal CM-2T at various stress amplitudes (τ_o) after $\gamma_p = 5 \times 10^{-3}$.

Figure 10. W_{irr} versus w_L (max) for crystal CM-IT at various prestrains.

Figure 11. $\bar{\tau}_F$ versus γ_p for crystals CM-IT and CM-Al.

Figure 12. τ^* versus $\bar{x}$ (schematic) for dislocations which experience the undulating long range internal stress field.

Figure 13. $\frac{\tau^* l}{\alpha G b}$ versus $\frac{\bar{x}}{2l}$ for the constant line tension approximation.

REFERENCES

(1). A. Seeger: Dislocations and Mechanical Properties of Crystals, 1957, John Wiley and Sons, p. 243.

(2). N. F. Mott: AIME Trans., 1960, vol. 218, p. 962.

(3). D. Kuhlmann-Wilsdorf: AIME Trans., 1962, vol. 224, p. 1047.

(4). Z. S. Basinski: Phil. Mag., 1959, vol. 4, p. 393.

(5). G. Saada: Electron Microscopy and Strength of Crystals, 1963, Interscience Pub., p. 651.

(6). H. Wiedersich: J. of Met., 1964, vol. 16, p. 425.

(7). A. Seeger, S. Mader and H. Kronmüller: Electron Microscopy and Strength of Crystals, 1963, Interscience Pub., p. 665.

(8). F. W. Young, Jr.: J. App. Phys., 1962, vol. 33, p. 963.

(9). F. W. Young, Jr.: J. App. Phys., 1961, vol. 32, p. 1815.

(10). J. Friedel: Electron Microscopy and Strength of Crystals, 1963, Interscience Pub., p. 616.

(11). R. F. Tinder and J. Washburn: Acta Met., 1964, vol. 12, p. 129.

(12). T. H. Blewitt: Phys. Rev., 1953, vol. 91, p. 1115.

(13). T. H. Blewitt, R. R. Coltman and J. K. Redman: Report on Confr. on Defects in Cryst. Sol., 1954, Phys. Soc., p. 369.

(14). A. R. Rosenfield and B. L. Averbach: Acta Met., 1960, vol. 8, p. 624.

(15). W. C. Overton, Jr., and J. Gaffney: Phys. Rev., 1955, vol. 98, p. 969.

(16). T. S. Liu, I. R. Kramer, and M. A. Steinberg: Acta Met., 1956, vol. 4, p. 364.

(17). J. Diehl and R. Berner: Z. Metallk., 1960, vol. 51, p. 522.

(18). I. R. Kramer: AIME Trans., 1959, vol. 215, p. 226.

(19). A. S. Nowick: Phys. Rev., 1950, vol. 80, p. 249.

(20). J. Weertman and J. S. Koehler: J. App. Phys., 1953, vol. 24, p. 624.

(21). R. R. Hasiguti and T. Hirai: J. App. Phys., 1951, vol. 22, p. 1084.

(22). A. S. Nowick: J. App. Phys., 1954, vol. 25, p. 1129.

(23). J. M. Roberts and D. E. Hartman: J. Phys. Soc. of Jap., 1963, vol. 18, supp. No. 1, p. 119.

(24). N. Brown and R. A. Ekvall: Acta Met., 1962, vol. 10, p. 1101.

(25). J. M. Roberts and D. E. Hartman: AIME Trans., in press.

(26). D. E. Hartman, D. A. Bresie and J. M. Roberts: Rev. Sci. Inst., 1963, vol. 34, p. 1272.

(27). J. M. Roberts and N. Brown: Acta Met., 1962, vol. 10, p. 430.

(28). M. S. Paterson: Acta Met., 1955, vol. 3, p. 491.

(29). S. Okuda and R. R. Hasiguti: Acta Met., 1963, vol. 11, p. 257.

(30). J. M. Roberts and N. Brown: AIME Trans., 1960, vol. 218, p. 454.

(31). P. R. Strutt: J. Aust. Inst. of Met., 1963, vol. 8, p. 115.

(32). J. Takamura and T. Morimoto: J. Phys. Soc. of Jap., 1963, vol. 18, supp. no. 1, p. 28.

(33). A. Ookawa and K. Yazu: Ibid, p. 36.

(34). H. G. van Bueren: Imperfections in Crystals, 1961, North Holland Pub. Co., Amsterdam, p. 152.

(35). G. Saada: Acta Met., 1961, vol. 9, p. 166.

(36). A. Seeger: Rep. Confr. on Defects in Crystl. Sol., 1955, Phys. Soc., p. 391.

(37). E. G. Shvidkovsky, E. P. Belozerova, and N. A. Tjapunina: J. Phys. Soc. of Jap., 1963, vol. 18, supp. No. 1, p. 161.

(38). G. Schoeck: Phil. Mag., 1964, vol. 9, p. 335.

(39). J. D. Livingston: Acta Met., 1962, vol. 10, p. 229.

(40). P. B. Hirsch: "Dislocation Distributions and Hardening Mechanisms in Metals," Jan. 1963, Nat. Phys. Lab. Symps., Teddington, Eng.

(41). G. Saada: Thesis, 1960, Faculty of Science, University of Paris.

(42). S. K. Mitra and J. E. Dorn: AIME Trans., 1962, vol. 225, p. 1062.

(43). D. Kuhlmann-Wilsodrf, H. J. Levinstein, W. H. Robinson, and H. G. F. Wilsdorf: J. Aust. Inst. Met., 1963, vol. 8, p. 102.

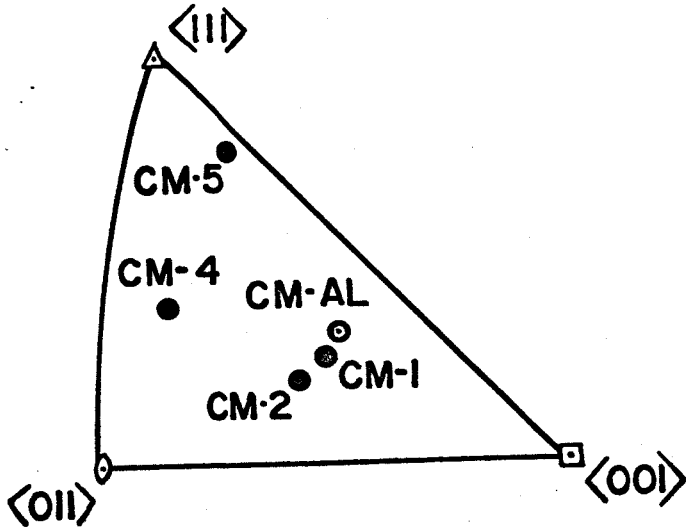

Figure 1

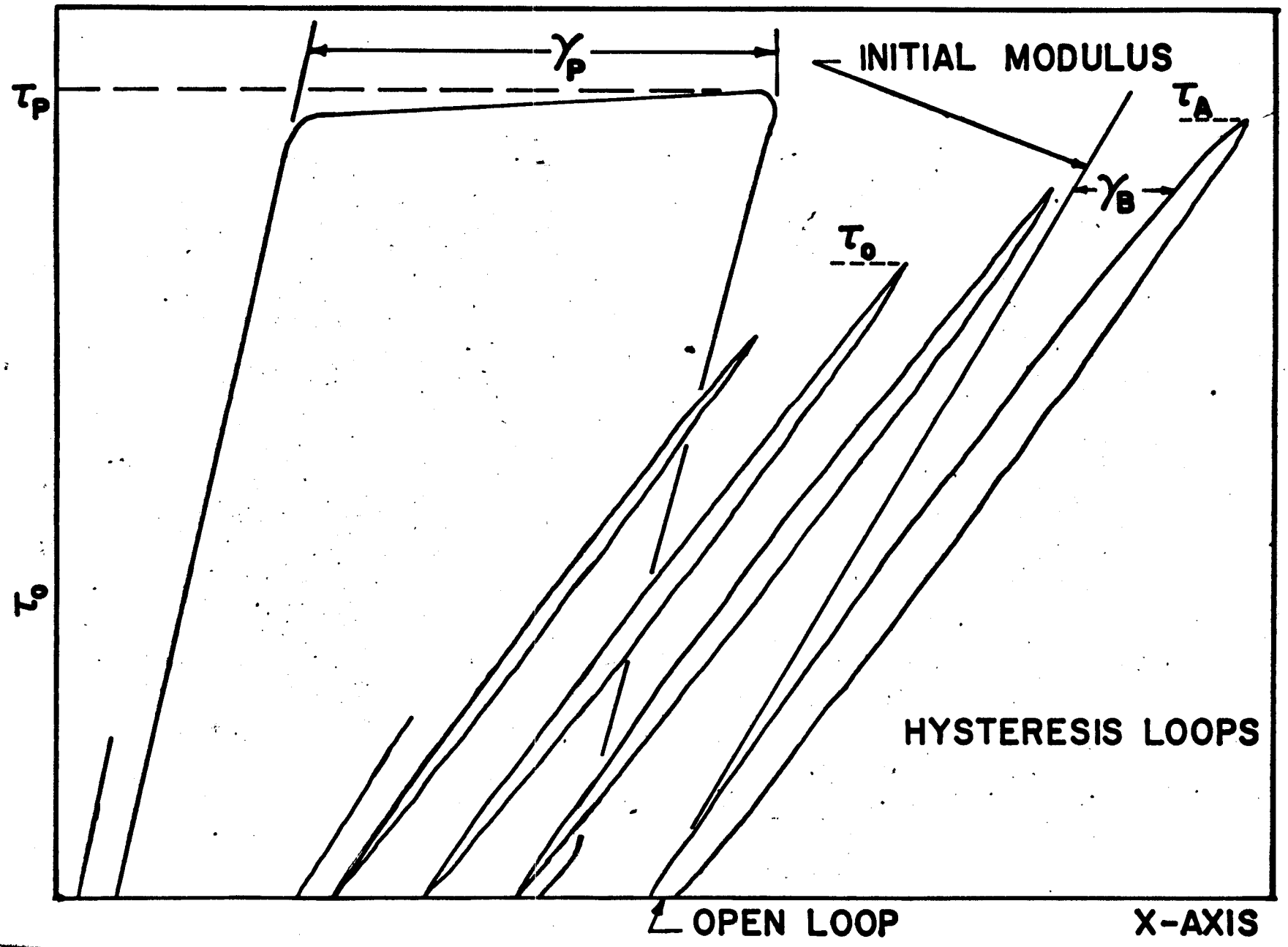
γ_p
INITIAL MODULUS
τ_p
τ_A
γ_B
τ_o
τ_o
HYSTERESIS LOOPS
OPEN LOOP
X-AXIS

Figure 2

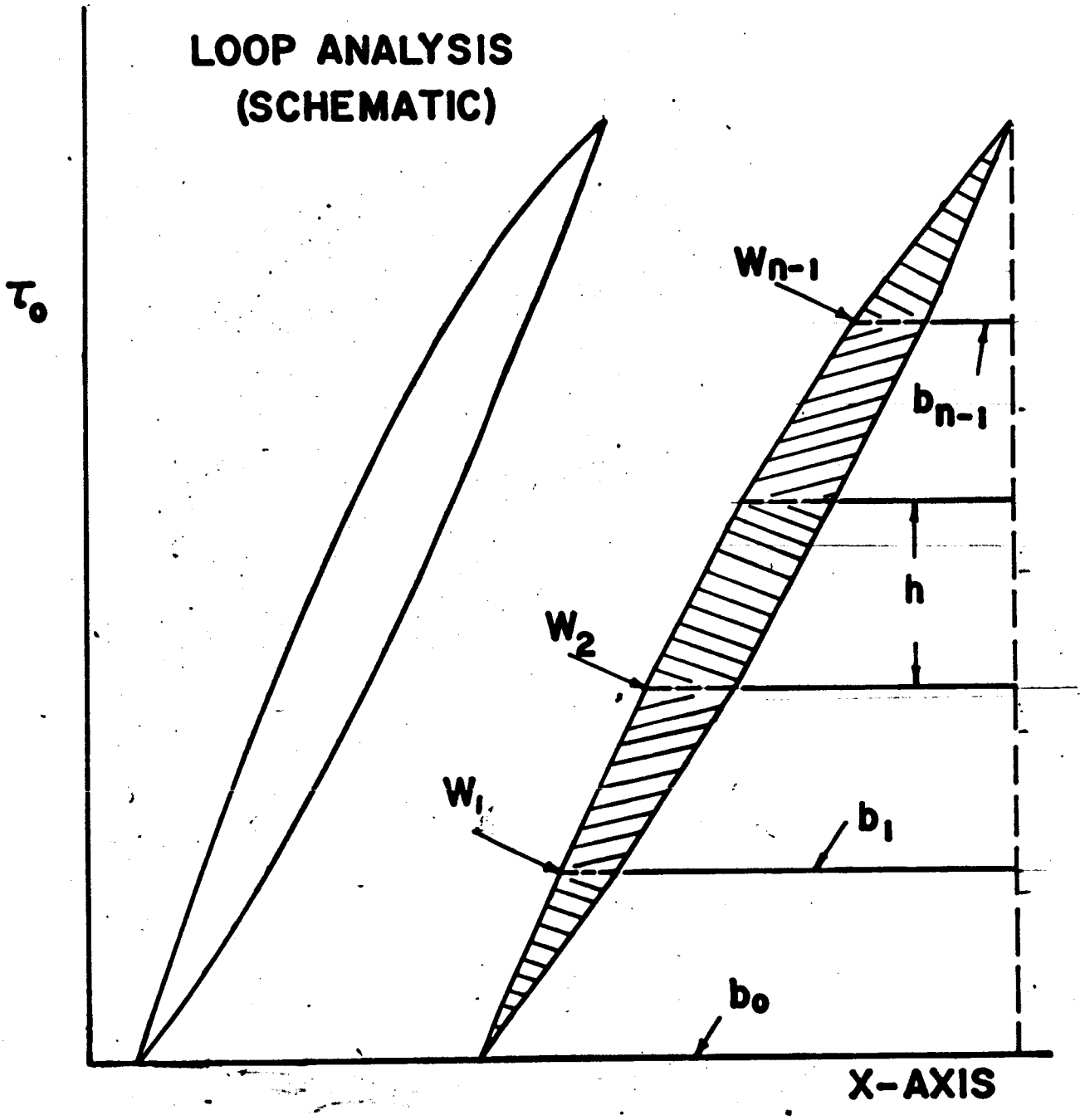

Figure 3

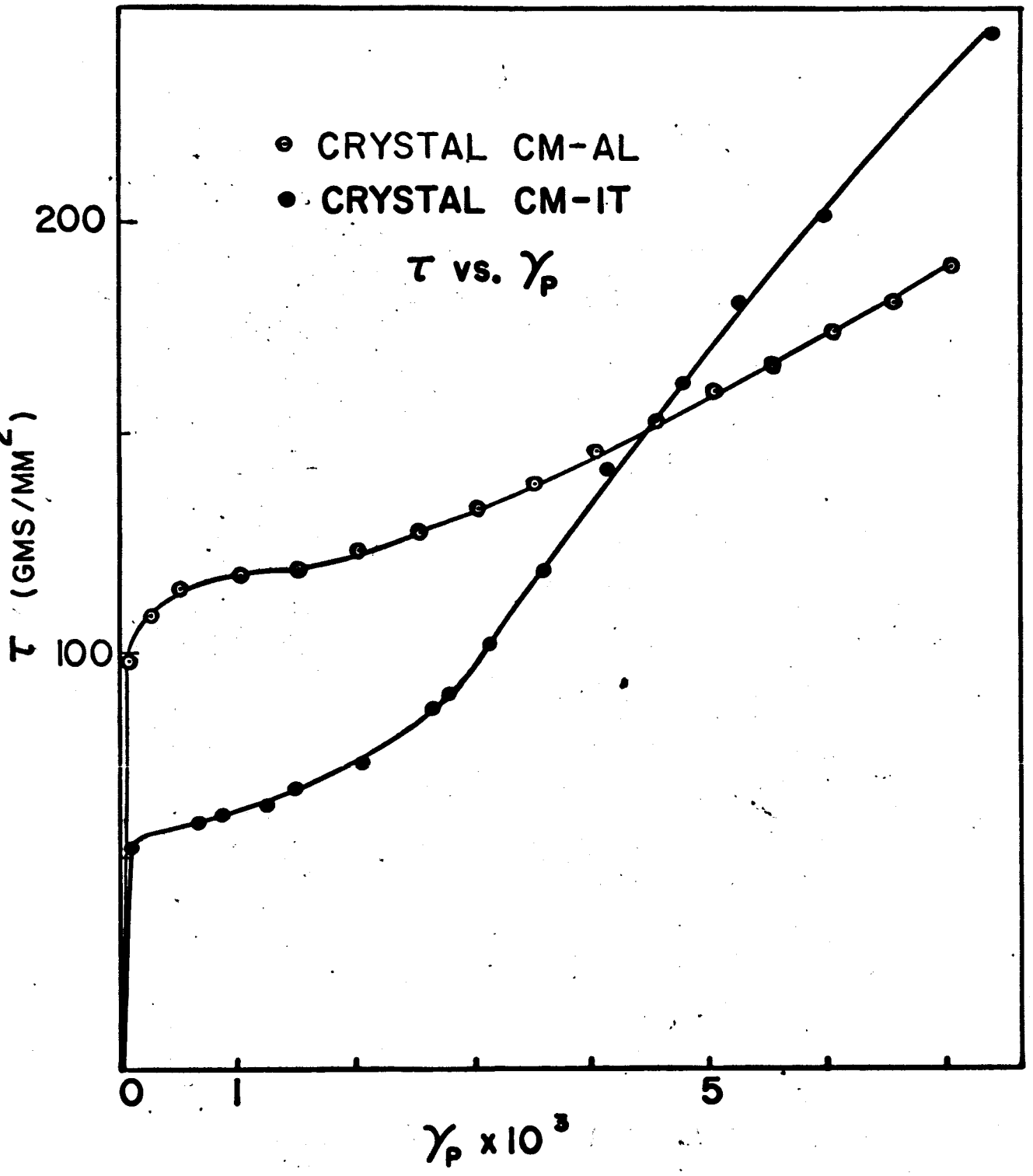

Figure 4

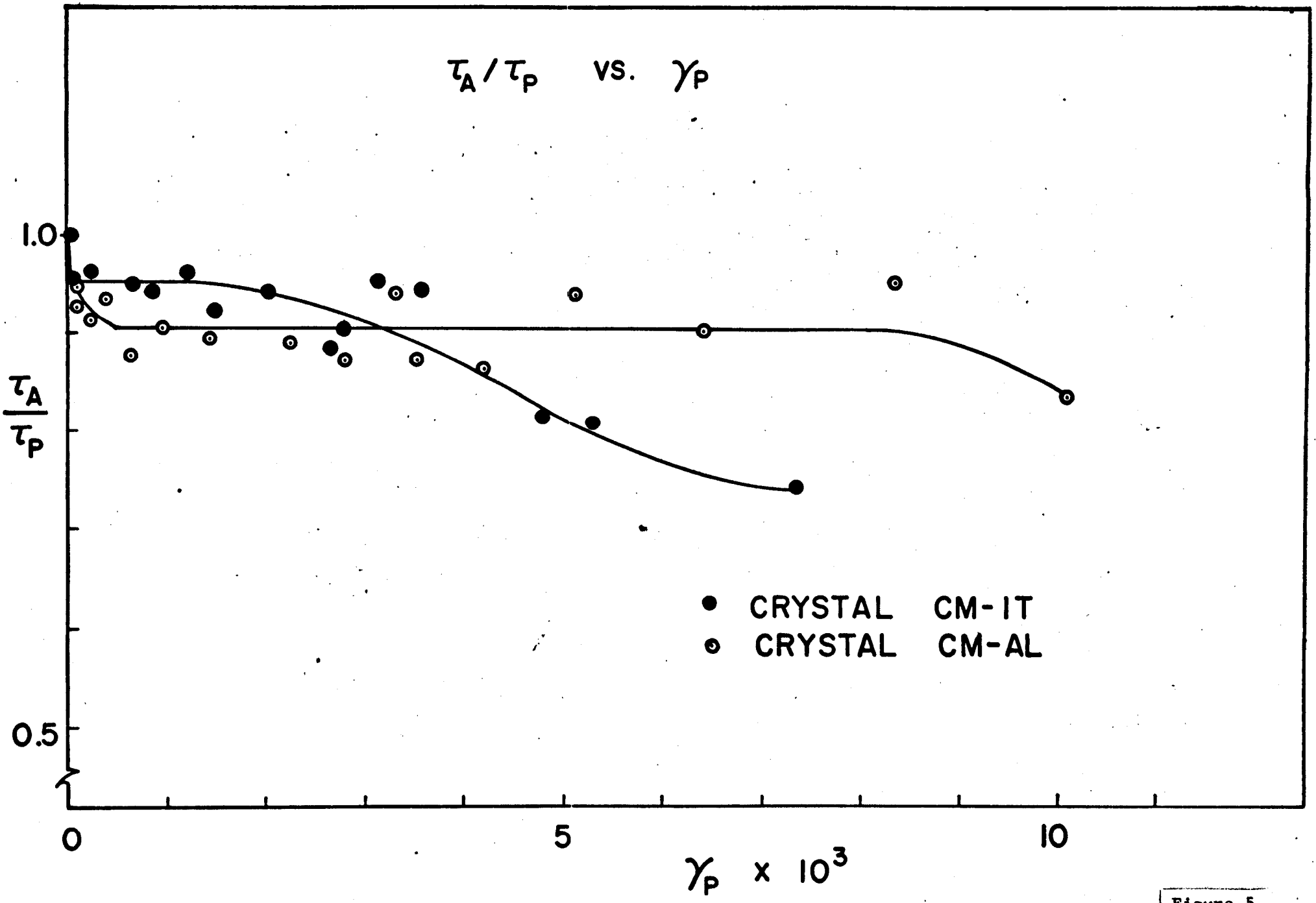
τ_A / τ_P vs. γ_P
1.0
0.5
$\frac{\tau_A}{\tau_P}$
CRYSTAL CM-IT
CRYSTAL CM-AL
0
5
10
$\gamma_P \times 10^3$

Figure 5

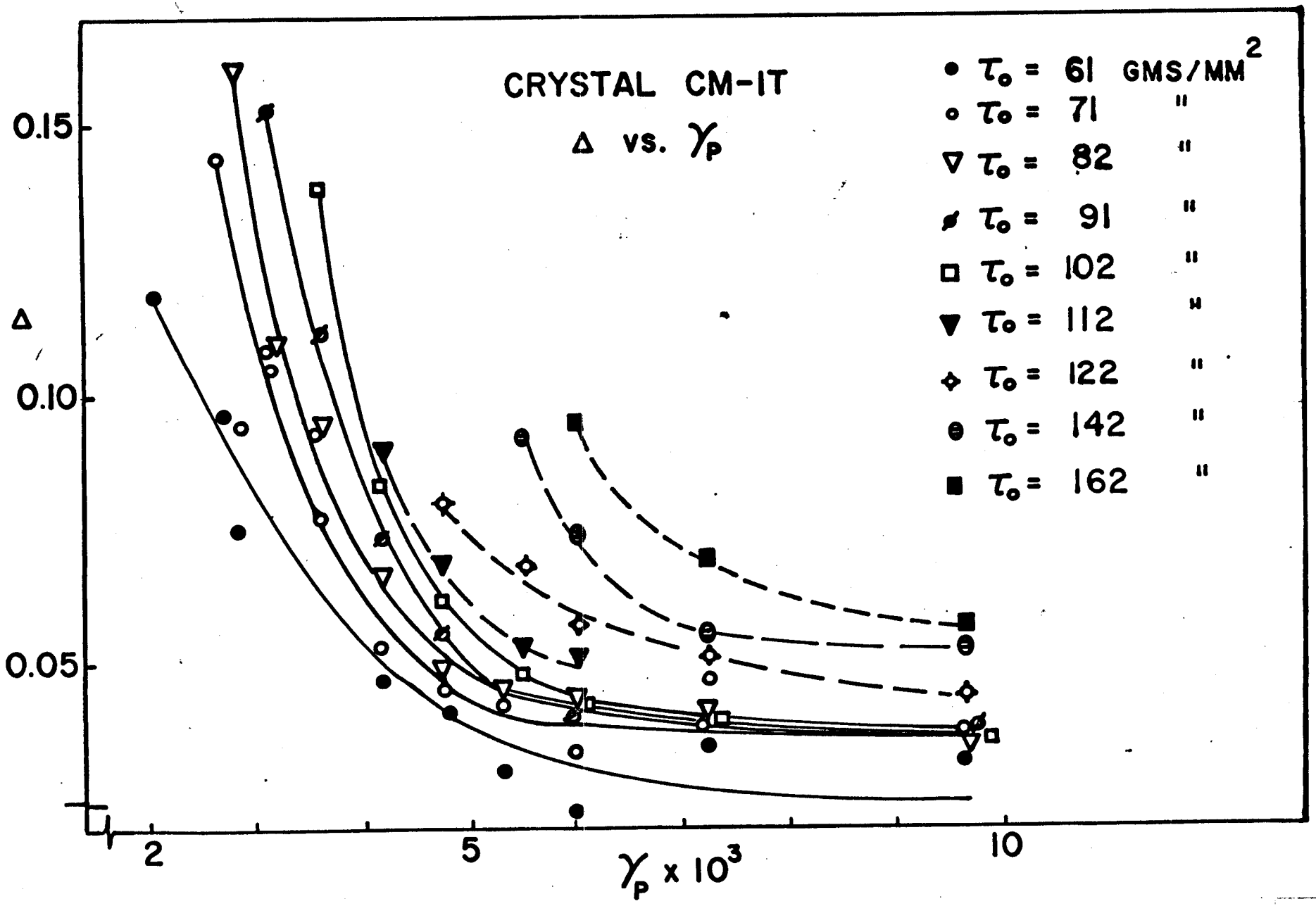
CRYSTAL CM-IT
Δ vs. γ_p
τ_o = 61 GMS/MM^2
τ_o = 71 "
τ_o = 82 "
τ_o = 91 "
τ_o = 102 "
τ_o = 112 "
τ_o = 122 "
τ_o = 142 "
τ_o = 162 "
0.15
0.10
0.05
Δ
2
5
10
γ_p x 10^3

Figure 6

Figure 7

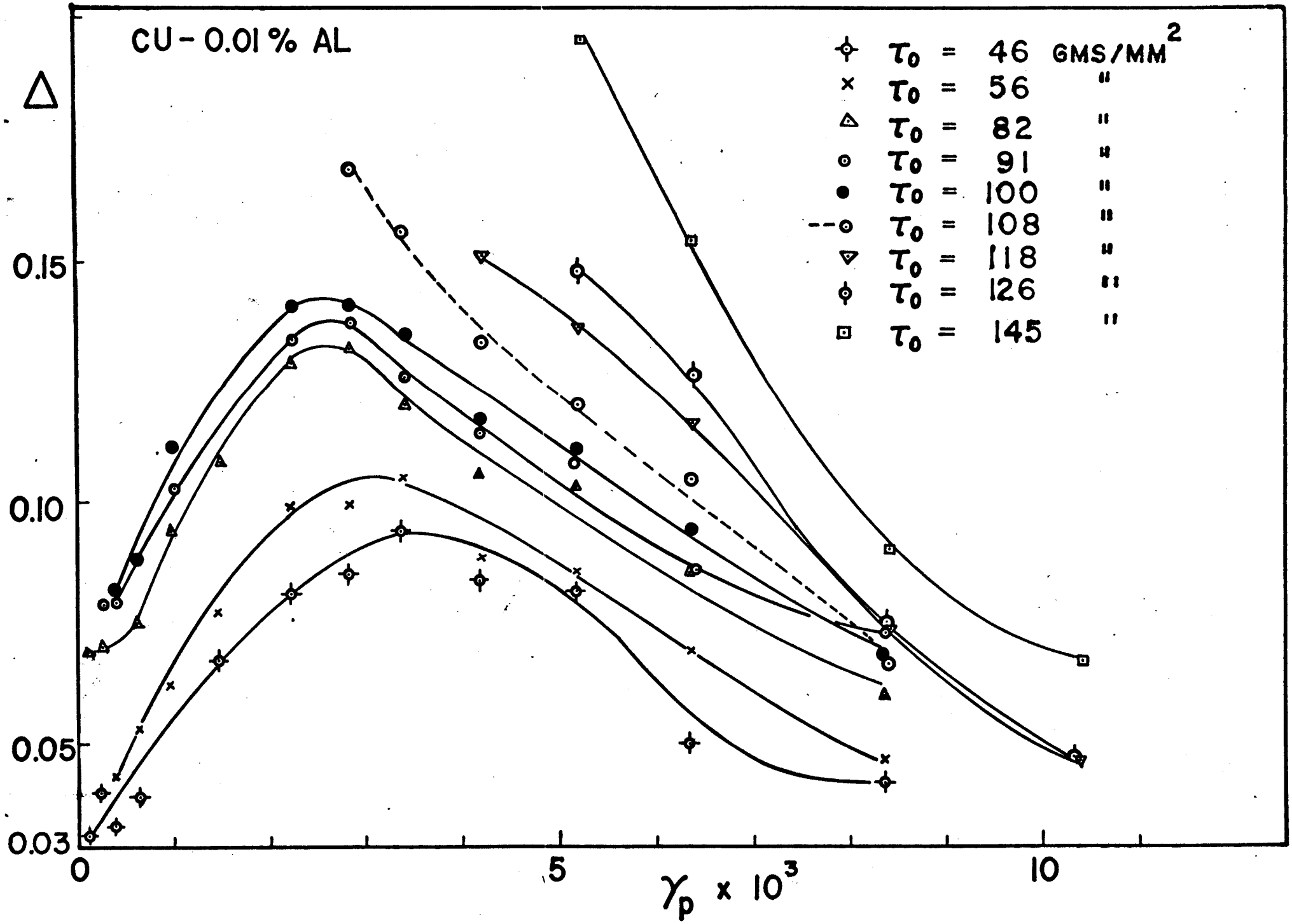
CU - 0.01 % AL
Δ
0.15
0.10
0.05
0.03
0
5
10
$\gamma_p \times 10^3$
τ_0 = 46 GMS/MM^2
τ_0 = 56 "
τ_0 = 82 "
τ_0 = 91 "
τ_0 = 100 "
τ_0 = 108 "
τ_0 = 118 "
τ_0 = 126 "
τ_0 = 145 "

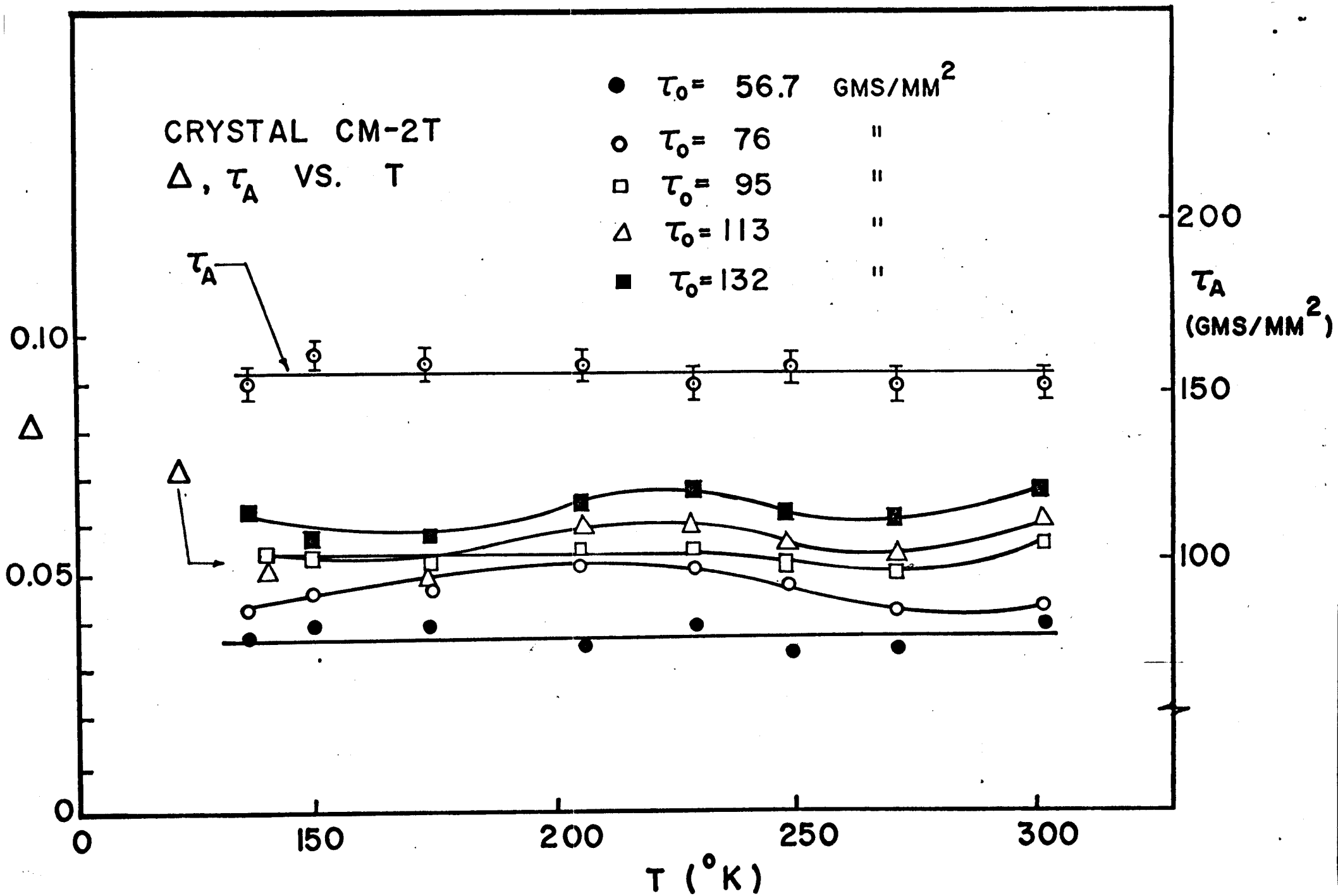
CRYSTAL CM-2T
Δ, τ_A VS. T
● τ_0= 56.7 GMS/MM^2
○ τ_0= 76 "
□ τ_0= 95 "
△ τ_0= 113 "
■ τ_0=132 "
τ_A
Δ
0.10
0.05
0
200
150
100
τ_A (GMS/MM^2)
0
150
200
250
300
T (°K)

Figure 8

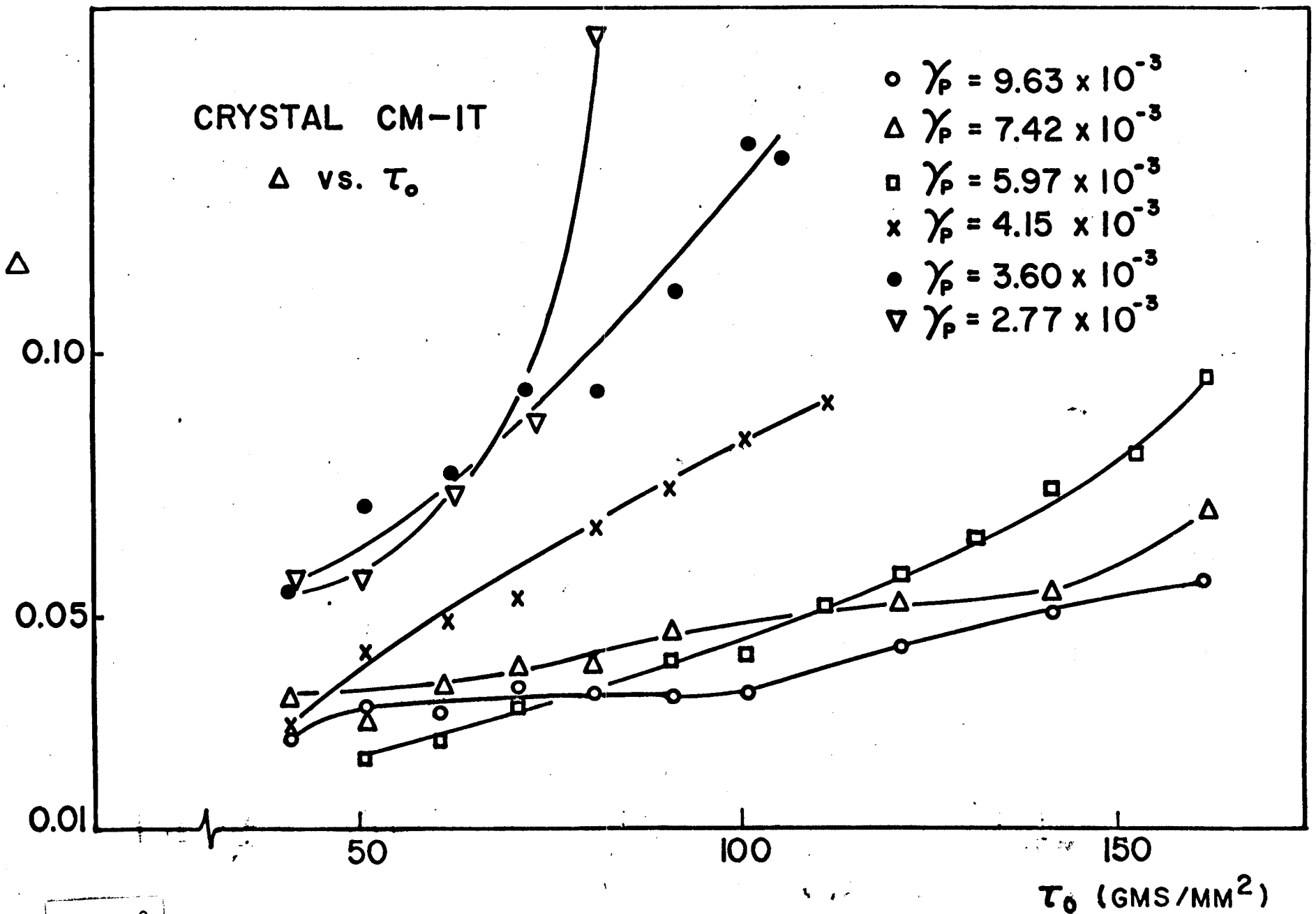
CRYSTAL CM-IT
Δ vs. τ_o
$\gamma_p = 9.63 \times 10^{-3}$
$\gamma_p = 7.42 \times 10^{-3}$
$\gamma_p = 5.97 \times 10^{-3}$
$\gamma_p = 4.15 \times 10^{-3}$
$\gamma_p = 3.60 \times 10^{-3}$
$\gamma_p = 2.77 \times 10^{-3}$
Δ
0.10
0.05
0.01
50
100
150
τ_o (GMS/MM^2)

Figure 9

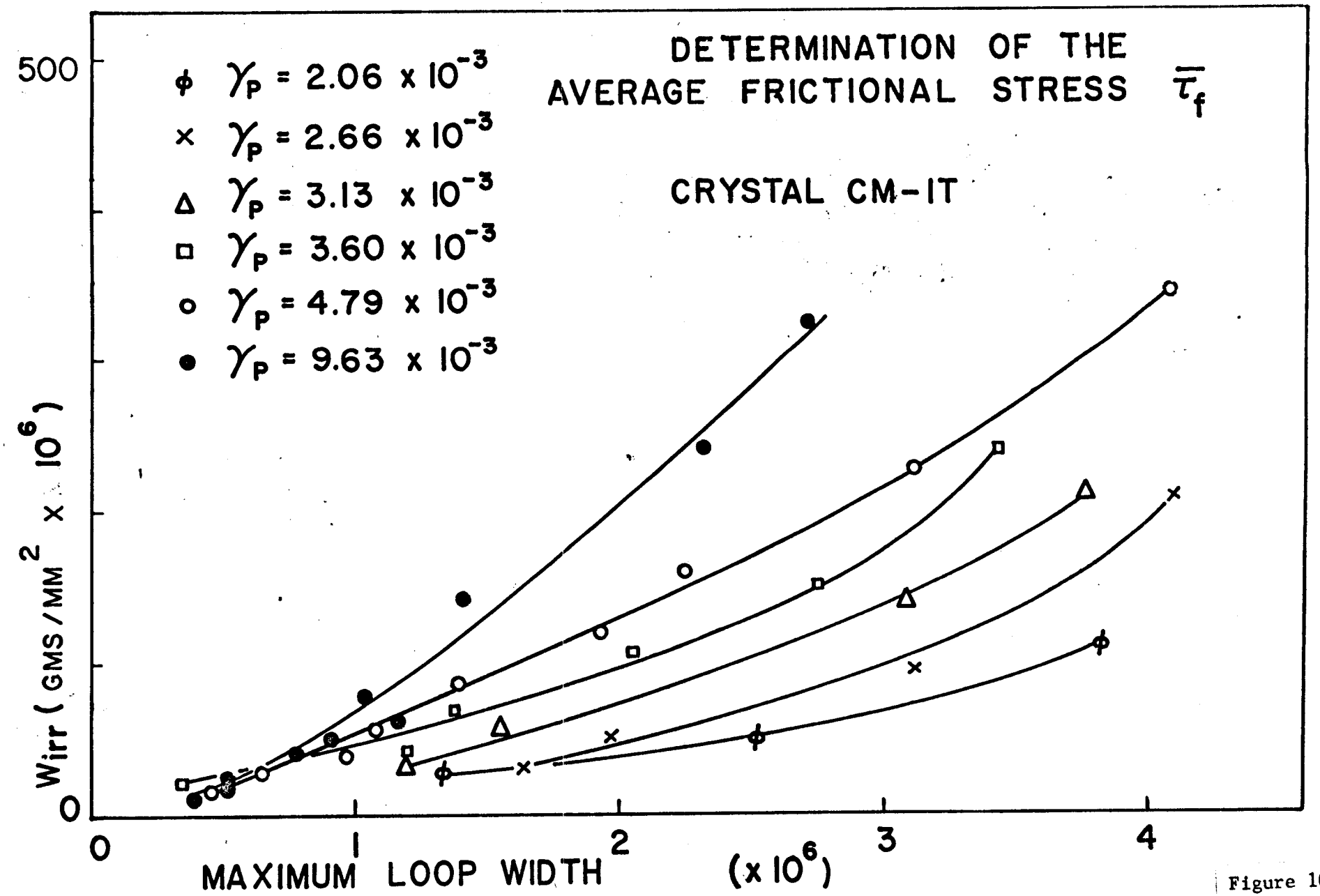
DETERMINATION OF THE
AVERAGE FRICTIONAL STRESS $\bar{\tau}_f$
CRYSTAL CM-IT
ϕ $\gamma_P = 2.06 \times 10^{-3}$
$\times$ $\gamma_P = 2.66 \times 10^{-3}$
Δ $\gamma_P = 3.13 \times 10^{-3}$
$\square$ $\gamma_P = 3.60 \times 10^{-3}$
$\circ$ $\gamma_P = 4.79 \times 10^{-3}$
$\bullet$ $\gamma_P = 9.63 \times 10^{-3}$
500
0
W_{irr} (GMS/MM^2 x 10^6)
0
1
2
3
4
MAXIMUM LOOP WIDTH^2 (x 10^6)

Figure 10

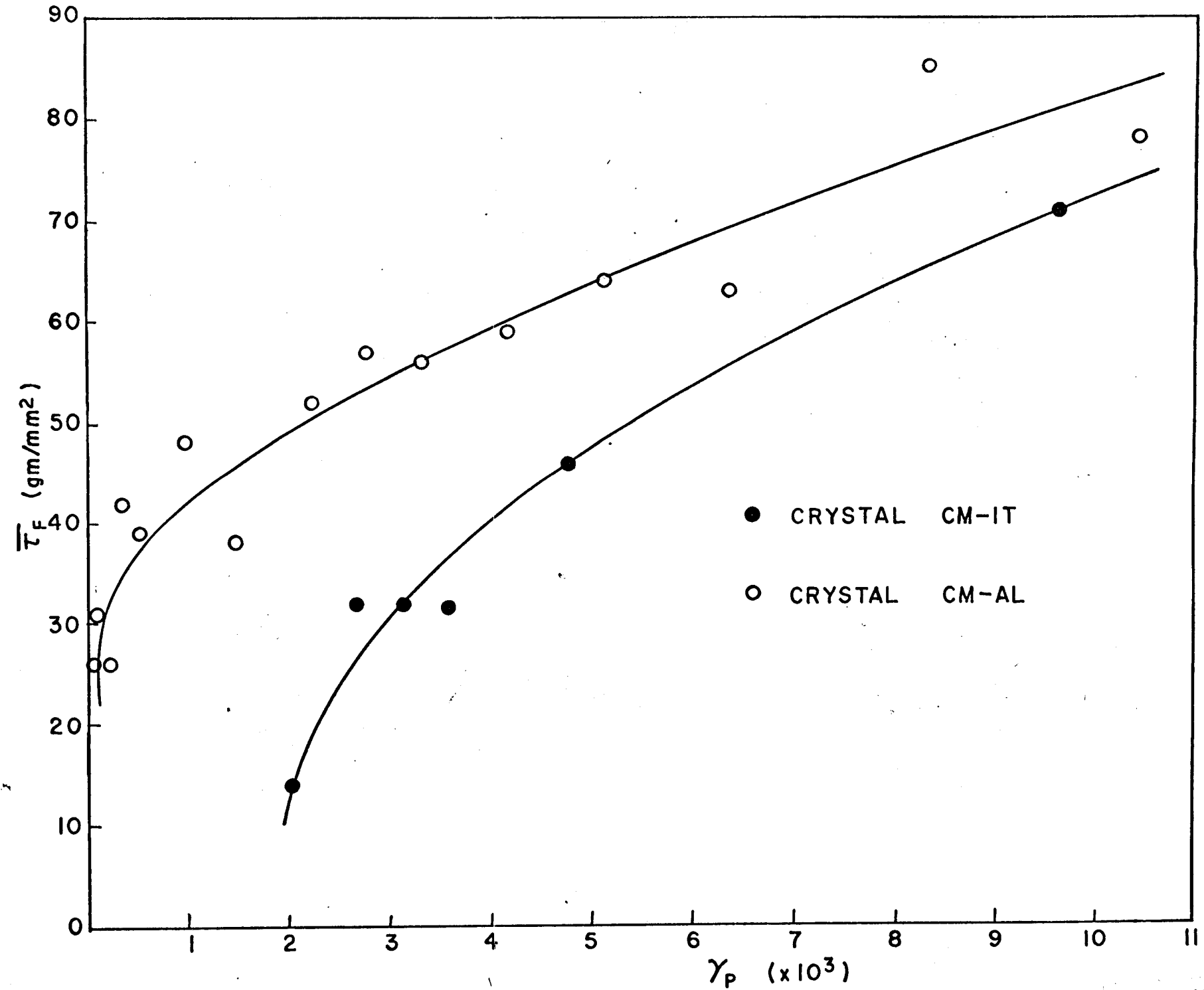
90
80
70
60
50
40
30
20
10
0
$\overline{\tau}_F$ (gm/mm²)
1
2
3
4
5
6
7
8
9
10
11
γ_p (x10³)
CRYSTAL CM-IT
CRYSTAL CM-AL

Figure 11

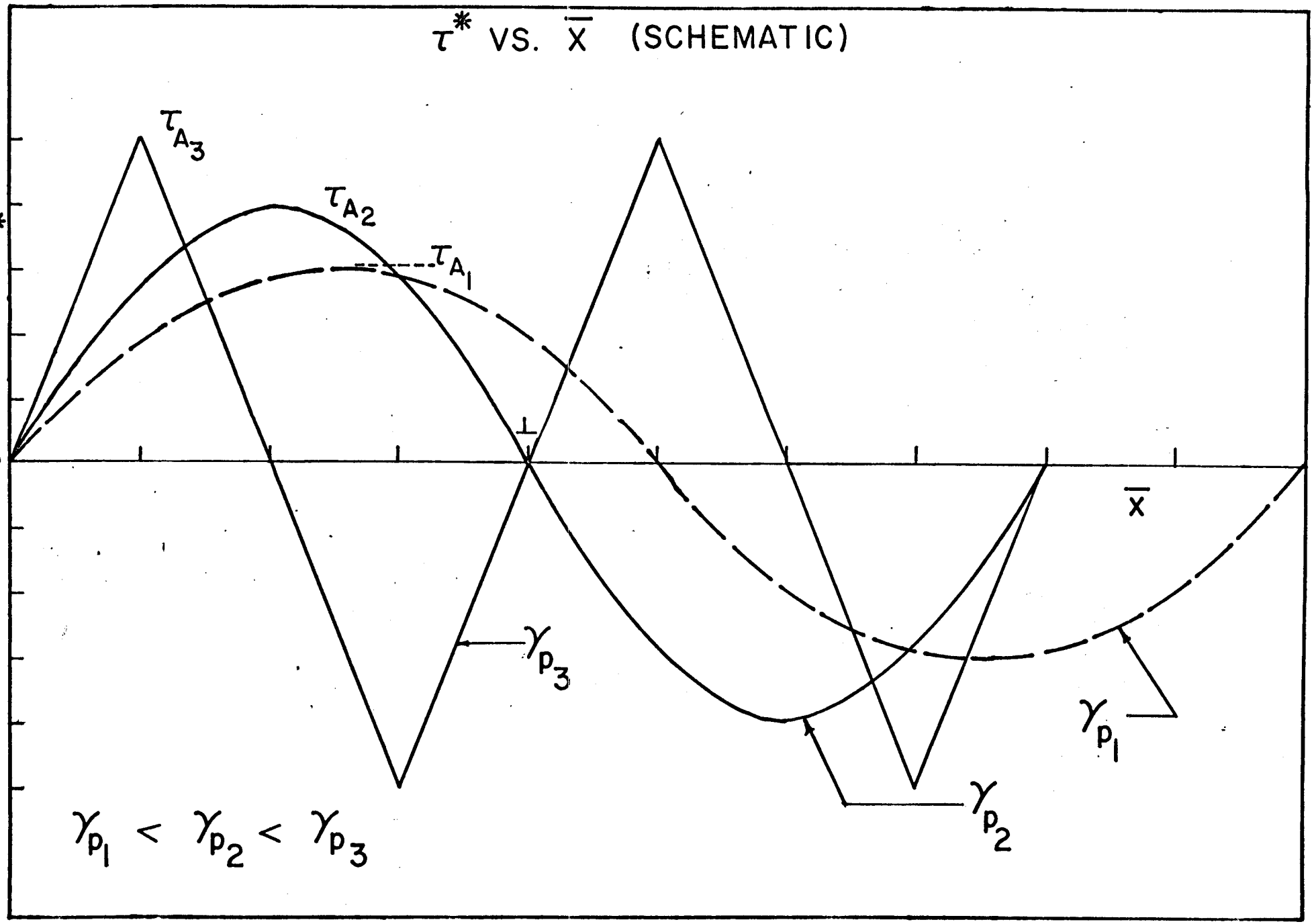
τ* VS. X̄ (SCHEMATIC)
τA3
τA2
τA1
τ*
(+)
0
(-)
⊥
X̄
γp3
γp2
γp1
γp1 < γp2 < γp3

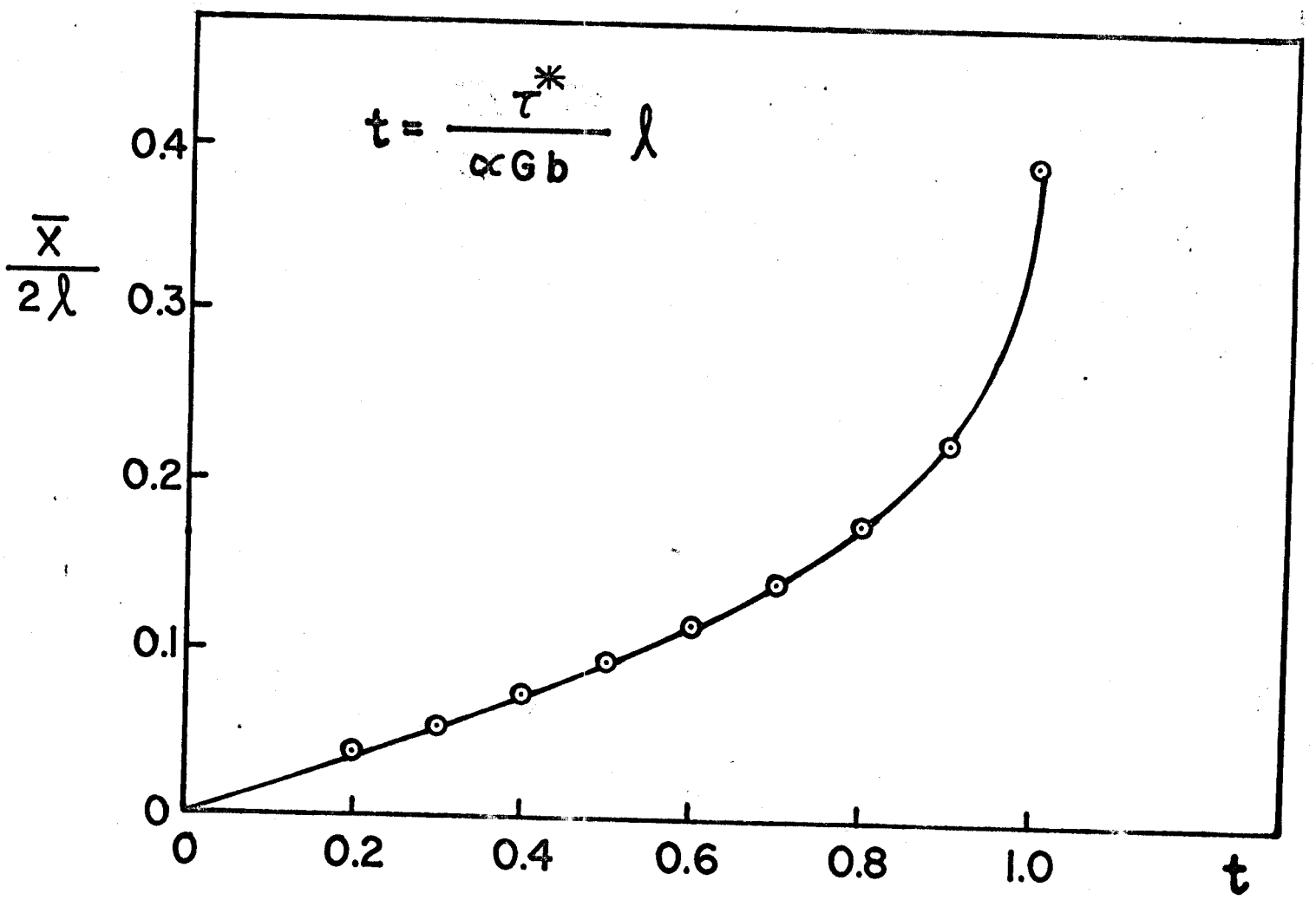

Figure 13